ISSN 1063-7834, Physics of the Solid State, 2015, Vol. 57, No. 4, pp. 675–682. © Pleiades Publishing, Ltd., 2015.
Original Russian Text © M.S. Pavlovskii, A.S. Shinkorenko, V.I. Zinenko, 2015, published in Fizika Tverdogo Tela, 2015, Vol. 57, No. 4, pp. 661–667.

DIELECTRICS

Calculation of Lattice Dynamics, Elastic and Dielectric Properties of γ-BiB_3O_6 and δ-BiB_3O_6

M. S. Pavlovskii*, A. S. Shinkorenko, and V. I. Zinenko

Kirensky Institute of Physics, Siberian Branch of the Russian Academy of Sciences, Akademgorodok 50–38, Krasnoyarsk, 660036 Russia

** e-mail: mspav@iph.krasn.ru*

Received October 10, 2014

Abstract—The crystal lattice vibration frequencies, densities of phonon states, elastic moduli, and high-frequency permittivities have been calculated in terms of the density functional theory method for two polymorphs γ-BiB_3O_6 and δ-BiB_3O_6. Based on the calculated densities of phonon states, the temperature dependences of the free energies of two considered bismuth triborate modifications have been constructed, and the temperature of the phase transition between these modifications has been determined (1100 K). The structure of a possible nonpolar praphase of δ-BiB_3O_6 has been proposed. The polarization of δ-BiB_3O_6 has been estimated as 131 μC/cm^2.

DOI: 10.1134/S1063783415040241

1. INTRODUCTION

Compound BiB_3O_6 (BBO) belongs to a family of borates that have attracted attention of researchers due to their high nonlinear optical properties [1]. Most of crystals of the family exist in several structural modifications depending on the conditions of their growth or external actions. In particular, bismuth triborate has six structural modifications [2, 3]. The structural basis of this compound is the boron–oxygen framework consisting of BO_4 tetrahedra or BO_4 tetrahedra and BO_3 triangles connected by their vertices [2, 3]. Bismuth atoms are arranged in the framework cavities (voids). It is known that only γ and δ modifications, among all bismuth triborate modifications, have structural frameworks consisting only of BO_4 tetrahedra (other modifications contain BO_4 tetrahedra and BO_3 triangles in proportion of 1 : 2 or 2 : 1 [2, 3]), and, as a result, these two modifications have highest densities which differ insignificantly in the γ and δ structures (6.177 and 6.378 g/cm^3, respectively). In [2], the constructed temperature/pressure BBO phase diagram demonstrates that the γ-BBO and δ-BBO modifications occupy the largest regions of the diagram. At zero pressure, δ-BBO exists in the range from low temperatures to 953 K and γ-BBO exists in the range from 953 K to 983 K; the melting temperatures of both modifications are the same (983 K). It was noted in [2] that the kinetics of phase transitions between the bismuth triborate modifications is very slow. For example, the γ-BBO phase is not formed in the sample bulk as the δ-BBO phase is annealed at temperatures of 923–973 K for 50 h. However, as a γ-BBO grain is added in the initial δ-BBO sample and the sample is subjected to annealing at temperatures of 953–983 K for 50 h, the γ-BBO phase occupies to 81% of the sample bulk.

The physical properties of bismuth triborate in the α modification [1, 2, 4, 5] have been studied extensively using experimental and theoretical methods. As for other modifications, most attention of researchers has been concentrated on the study of their optical properties. At the same time, for example, to reveal the physical cause of a large nonlinear optical coefficient in δ-BBO or its high mechanical strength, it is very important to know the phonon spectra, the elastic moduli, and the piezoelectric response. In [6], the limiting crystal lattice vibration frequencies of δ-BBO were determined experimentally by Raman and IR spectroscopy and these frequencies were calculated in a model using the interatomic potentials, whose parameters were fit using the experimental data. Several values of the limiting vibration frequencies of γ-BBO, which were obtained experimentally using Raman spectroscopy, are given in [3].

This work is devoted to the ab initio calculation of the phonon spectra, dielectric and elastic properties of the γ and δ modifications of the BiB_3O_6 crystal.

2. RESULTS OF CALCULATIONS

The spectra of the crystal lattice vibration frequencies, the high-frequency permittivity, the dynamic Born charges, and the elastic moduli were calculated in the framework of the ab initio model of an ionic crystal with inclusion of the dipole and quadrupole polarizabilities of the ions. The model was described in detail in [7].

Table 1. Lattice parameters and fractional atomic coordinates of δ-BBO with symmetry space group $Pca2_1$ according to the experimental data [8] and the theoretical calculation (given in the parentheses)

Atom	Wyckoff position	x	y	z
Bi	4*a*	0.8379 (0.830)	0.1574 (0.168)	0.2024 (0.196)
O(1)	4*a*	0.7883 (0.787)	0.3102 (0.313)	0.1578 (0.196)
O(2)	4*a*	0.9394 (0.940)	0.3611 (0.362)	0.0695 (0.073)
O(3)	4*a*	0.8543 (0.854)	0.7600 (0.762)	0.0338 (0.036)
O(4)	4*a*	0.7242 (0.724)	0.7487 (0.752)	−0.0133 (−0.011)
O(5)	4*a*	0.0679 (0.068)	0.2639 (0.263)	−0.0247 (−0.022)
O(6)	4*a*	0.9821 (0.983)	0.8710 (0.871)	−0.0274 (−0.024)
B(1)	4*a*	0.7871 (0.787)	0.6369 (0.639)	0.1678 (0.169)
B(2)	4*a*	0.9277 (0.928)	0.6730 (0.674)	0.1456 (0.148)
B(3)	4*a*	0.0023 (0.003)	0.1759 (0.176)	0.1144 (0.117)
	V	a	b	c
Lattice parameters	351.37 Å^3 (333.91 Å)	18.4480 Å (18.3034 Å)	4.4495 Å (4.3378 Å)	4.2806 Å (4.2056 Å)

Table 2. Lattice parameters and fractional atomic coordinates of γ-BBO with symmetry space group $P2_1/c$ according to the experimental data [8] and the theoretical calculation (given in parentheses)

Atom	Wyckoff position	x	y	z
Bi	4*e*	0.1563 (0.167)	0.615 (0.598)	0.3702 (0.361)
O(1)	4*e*	0.846 (0.847)	0.624 (0.624)	0.879 (0.880)
O(2)	4*e*	0.778 (0.780)	0.578 (0.577)	0.554 (0.555)
O(3)	4*e*	0.792 (0.793)	0.772 (0.773)	0.670 (0.671)
O(4)	4*e*	0.335 (0.337)	0.658 (0.659)	0.717 (0.719)
O(5)	4*e*	0.346 (0.347)	0.879 (0.880)	0.546 (0.548)
O(6)	4*e*	0.809 (0.809)	0.967 (0.968)	0.685 (0.686)
B(1)	4*e*	0.702 (0.674)	0.658 (0.659)	0.693 (0.693)
B(2)	4*e*	0.713 (0.694)	0.868 (0.869)	0.564 (0.564)
B(3)	4*e*	0.181 (0.202)	0.583 (0.584)	0.867 (0.868)
	β	a	b	c
Lattice parameters, $V = 362.83$ Å^3	91.0689° 90°	4.2596 Å (4.1421 Å)	11.7093 Å (11.5587 Å)	7.2757 Å (7.2209 Å)

The δ-BBO modification has a polar structure with symmetry space group $Pca2_1$ with four molecules in the unit cell [8] (the lattice parameters and fractional atomic coordinates are given in Table 1). The γ-BBO modification has the centrosymmetric structure with symmetry space group $P2_1/n$ and also with four molecules in the unit cell [9]. Note that the γ-BBO structure is described in [9] using a nonstandard installation for the monoclinic symmetry group, in which the angle of monoclinicity is 121.141°. We use the standard installation with symmetry space group $P2_1/c$. The lattice parameters and the fractional atomic coordinates in this installation obtained using the FINDSYM program [10] are given in Table 2. In this installation, the angle of monoclinicity is 91.0689°, i.e., it is very close to the right angle. We calculated the vibration frequency spectrum over the Brillouin zone in γ-BBO, using for convenience angle 90°, which leads to insignificant (less than 1%) differences of the frequencies, according to the comparison with the vibration frequencies in the Brillouin zone center calculated for the angles of monoclinicity 91.0689° and 90°.

The calculation of the vibration frequency spectrum for the γ-BBO and δ-BBO crystal lattices using the experimental values of the lattice parameters and the atomic coordinates shows the existence of instable vibrational modes.

To eliminate the instable modes, we perform the relaxation of the structures of both the modifications with respect to the lattice parameters and the atomic coordinates. The lattice parameters and the fractional atomic coordinates obtained as a result of the relaxation are listed in Tables 1 and 2. As is seen from the Tables, the calculated lattice parameters differ from the experimental parameters by not larger than 3%, and the largest difference between the relaxed and experimental fractional atomic coordinates is 1%.

The expansion of the total oscillation representation in the Brillouin zone center for the γ phase has the following view: $\Gamma = 30A_g + 30B_g + 30A_u + 30B_u$, where

Table 3. Vibration frequencies (cm^{-1}) in the Brillouin zone center of the γ-BBO crystal and oscillator strengths S of the corresponding IR-active modes according to the calculation performed in this work

A_g	B_g	A_u (LO)	A_u (TO)	S	B_u (LO_x)	B_u (LO_z)	B_u (TO)	S_x	S_y
1093	1121	1111	1089	0.136	1178	1087	1087	0.623	0.000
1024	1066	1075	1072	0.019	1038	1063	1035	0.021	0.187
946	1029	1023	982	0.293	1006	1009	1006	0.000	0.018
928	926	982	936	0.350	957	965	948	0.070	0.123
887	904	931	891	0.319	899	886	871	0.234	0.122
774	839	886	794	0.848	857	867	855	0.019	0.104
715	748	763	752	0.102	728	855	709	0.191	1.564
687	682	700	696	0.034	702	703	698	0.047	0.049
670	656	641	636	0.064	671	659	656	0.158	0.029
589	590	584	584	0.000	624	597	593	0.370	0.048
539	571	561	558	0.045	591	578	569	0.378	0.116
525	520	550	543	0.091	534	525	517	0.242	0.112
507	499	508	503	0.068	508	507	506	0.029	0.020
484	474	492	490	0.028	503	485	480	0.340	0.076
444	448	486	479	0.104	467	466	466	0.014	0.011
423	429	438	438	0.003	451	451	448	0.052	0.039
422	415	421	421	0.000	411	408	407	0.074	0.006
379	385	399	399	0.006	399	400	399	0.003	0.014
351	333	369	369	0.005	368	372	361	0.139	0.216
337	319	348	347	0.014	352	351	351	0.036	0.007
305	314	320	320	0.001	330	330	329	0.021	0.023
285	288	300	299	0.005	304	303	301	0.079	0.053
265	262	257	254	0.078	274	272	272	0.058	0.002
231	257	214	214	0.000	223	225	222	0.014	0.093
207	209	188	183	0.177	196	205	194	0.094	0.430
149	183	164	164	0.013	159	162	134	1.438	1.625
123	174	127	100	2.083	98	119	93	0.352	2.110
93	120	56	55	0.054	24	47	24	0.143	10.227
66	78	48	45	0.384					
53	39								

the acoustic modes are $A_u + 2B_u$ modes. Modes A_g and B_g are Raman-active, and modes A_u and B_u are IR-active. The calculated limiting vibration frequencies for γ-BBO are given in Table 3.

The expansion of the total oscillation representation in the Brillouin zone center for the δ phase has the following view: $\Gamma = 30A_1 + 30A_2 + 30B_1 + 30B_2$, including acoustic modes $A_1 + B_1 + B_2$. Optical modes A_1, B_1, and B_2 are active in the Raman spectra and IR spectra. Modes A_2 are Raman-active.

The limiting vibration frequencies of δ-BBO calculated in this work are given in Tables 4 and 5; the Tables also contain, for comparison, the limiting frequencies obtained in [6], where the frequencies obtained from the Raman spectra are classified by irreducible representations, and the IR-active modes are given without classification.

In this work, we calculated the moduli of elasticity (GPa)

for γ-BBO

$$C_\gamma = \begin{bmatrix} 328.2 & 83.3 & 155.5 & 0 & 6.3 & 0 \\ 83.3 & 411.4 & 83.4 & 0 & -3.0 & 0 \\ 155.5 & 83.4 & 313.1 & 0 & 0.1 & 0 \\ 0 & 0 & 0 & 76.9 & 0 & -3.0 \\ 6.3 & -3.0 & 0.1 & 0 & 151.7 & 0 \\ 0 & 0 & 0 & -3.0 & 0 & 79.5 \end{bmatrix}, \quad (1)$$

Table 4. Vibration frequencies (cm^{-1}) of the IR- and Raman-active modes in the Brillouin zone center of the δ-BBO crystal according to the measurements in [6] and the theoretical calculation in this work (the oscillator strengths S of the A_1-type modes are calculated in this work)

A_1	A_1	A_1	A_1	A_1	A_2	A_2	IR
calc.	calc.	calc.	exper.	exper.	calc.	exper.	exper.
LO	TO	S	LO	TO	TO	TO	
1112	1105	0.047		1113	1105	1075	1263
1063	1031	0.237	1075	1075	1031	1031	1120
1022	1004	0.135	1031	1030	1015	1008	1085
986	986	0.000	1006	996	986	975	1044
945	923	0.182	974	954	926	935	1006
908	881	0.235	935	895	880	863	960
792	772	0.198	784	863	866	783	937
765	727	0.394	727	783	792	727	928
642	636	0.071	647	753	714	708	887
584	582	0.030	607	726	632	648	818
582	536	0.666	530	639	544	607	791
512	511	0.015	515	607	524	530	770
500	498	0.040	501	530	498	514	744
489	475	0.218	467	515	478	501	726
458	453	0.083	417	499	456	467	703
434	431	0.042	402	467	435	417	644
394	392	0.044	395	415	406	401	627
375	374	0.011	329	395	401	394	607
366	366	0.000	314	327	373	329	578
330	330	0.000	256	304	357	314	568
309	305	0.085	247	246	326	255	531
283	283	0.000	228	228	301	246	499
268	268	0.000	206	206	294	228	488
230	230	0.008	195	185	252	205	467
188	166	1.066	170	177	247	196	416
144	139	0.255	150	124	227	170	403
115	114	0.023	124	115	86	124	393
87	48	8.327	116	99	71	115	367
26	23	1.194	109		63	108	328
					57		311
							257
							242
							205
							190
							173
							154
							127
							119

and for δ-BBO

$$C_\delta = \begin{bmatrix} 363.9 & 127.0 & 120.7 & 0 & 0 & 0 \\ 127.0 & 361.3 & 111.5 & 0 & 0 & 0 \\ 120.7 & 111.5 & 365.5 & 0 & 0 & 0 \\ 0 & 0 & 0 & 108.2 & 0 & 0 \\ 0 & 0 & 0 & 0 & 117.7 & 0 \\ 0 & 0 & 0 & 0 & 0 & 124.1 \end{bmatrix}. \quad (2)$$

The calculated values of the high-frequency permittivity and the moduli of dilatation of both considered bismuth triborate modifications are listed in Table 6.

Figure 1 shows the calculated total and partial densities of phonon states of bismuth, boron, and oxygen atoms for γ-BBO and δ-BBO.

3. DISCUSSION OF THE RESULTS

As is seen from Eqs. (1), (2), and Table 6, the values of elastic moduli C_{ij} and the bulk modulus in γ-BBO and δ-BBO differ insignificantly; it is not surprise, because both the structures have the same structural frameworks and close interatomic distances (the maximum difference of the interatomic distances in these structures is 3%). We did not find available experimental data on elastic moduli for neither γ-BBO nor δ-BBO, and, because of this, did not compare the calculated and experimental values. It is seen from Table 6 that the values of the high-frequency permittivity tensor components also differ insignificantly, and the refractive indices agree adequately with the measured values [11, 12].

Unfortunately, we had not possibility to compare the calculated limiting vibration frequencies for γ-BBO (Table 3) with experimental data, because there are no available detailed experimental data on the phonon spectra of γ-BBO. In [3], the authors present the Raman spectrum of γ-BBO, indicating only the frequencies 430, 473, 548, 602, 701, and 1055 cm^{-1} without their classification.

It is seen from Tables 4 and 5 that the limiting frequencies of δ-BBO calculated in this work agree well with the experimental data; the main difference can be observed at low frequencies, but the frequencies lower than 100 cm^{-1} were not likely to be observed experimentally. Among the calculated vibrational modes, there are two modes with highest frequencies: the B_1-type mode with a frequency of 1203/1157 cm^{-1} (LO/TO) and the B_2-type mode with a frequency of 1204/1203 cm^{-1} (LO/TO). There are no modes with such frequencies in the experimental Raman spectra; however, there are two modes with highest frequencies 1263 cm^{-1} and 1120 cm^{-1} among the IR-active modes.

We estimated the oscillator strength of the mode [13]

$$S_i = \varepsilon_\infty \frac{\omega^2_{\mathrm{LO},i} - \omega^2_{\mathrm{TO},i}}{\omega^2_{\mathrm{TO},i}}. \quad (3)$$

for the calculated frequencies of the A_1, B_1, and B_2 types in δ-BBO and A_u and B_u in γ-BBO. The oscillator strengths calculated by Eq. (3) are given in Tables 3, 4, and 5.

In the γ-BBO crystal, the modes with frequencies (LO/TO) 47/24, 119/93, 127/100, 162/134, 855/709, 159/134, 886/794, 1178/1087 cm^{-1} have the highest oscillator strengths 10.227, 2.110, 2.083, 1.625, 1.564, 1.438, 0.848, and 0.623, respectively. In the δ-BBO crystal, modes with frequencies (LO/TO) 87/48, 126/80, 92/61, 63/43, 209/177, 26/23, 188/166, 1136/1045, and 582/536 cm^{-1} have the highest oscillation strengths 8.327, 5.221, 4.507, 3.940, 1.430, 1.194, 1.066, 0.655, and 0.666, respectively. The high oscillator strengths of the low-frequency modes (lower than 200 cm^{-1}) correspond to polar oscillation modes, in eigenvectors of which positively charged bismuth ions are displaced in one direction and negatively charged oxygen ions are displaced in the opposite direction. At high frequencies, bismuth ions do not almost participate in the lattice vibrations, and high oscillator strengths correspond to the modes, in eigenvectors of which most of boron ions are displaced in one direction and most of oxygen ions are displaced in the opposite direction. In [6], the oscillator strengths were estimated for the measured A_1-type modes; the largest of them 0.09, 0.22, 0.12, 0.29, 0.54, 1.257 correspond to frequencies 996, 954, 639, 304, 185, and 99 cm^{-1}, respectively; the estimation shows that low-frequency modes have the largest oscillator strengths.

Let us discuss the stability of the δ-BBO and γ-BBO phases as temperature varies. As was already noted in Section 1, the experimental studies showed that the δ phase is most stable at low temperatures, and the γ phase becomes more stable at temperatures higher than 950 K [2]. Our calculations show that, at $T = 0$ K, the δ phase is more energetically favorable as compared to the γ phase; however, the total energies of these phases are close, as is seen from Table 7 that gives the total energy (less the ion intrinsic energy) and individual contributions in these energies for δ-BBO and γ-BBO. The proximity of the energies of the δ and γ phases at zero temperature allow us to suppose that, at a finite temperature, the γ phase becomes more stable as compared to the δ phase due to the phonon contribution to the free energy. In this work, we used the expression for the free energy in the harmonic approximation [14], assuming that anharmonic contributions of the γ and δ phases to $F(T)$ are the same:

$$F(T) = E_{\mathrm{static}} + F_{\mathrm{vibr}}(T), \quad (4)$$

Table 5. Vibration frequencies (cm^{-1}) of the IR- and Raman-active modes in the Brillouin zone center of the δ-BBO crystal according to the measurements in [6] and the theoretical calculation in this work (the oscillator strengths S of the B_1- and B_2-type modes are calculated in this work)

B_1	B_1	B_1	B_1	B_2	B_2	B_2	B_2	IR
calc.	calc.	calc.	exper.	calc.	calc.	calc.	exper.	exper.
LO	TO	S	TO	LO	TO	S	TO	
1203	1157	0.287	1079	1204	1203	0.009		1263
1045	1042	0.015	1032	1136	1045	0.655	1082	1120
1025	1019	0.040	998	1024	1014	0.069	1028	1085
988	961	0.205	934	1007	990	0.126	996	1044
924	915	0.068	919	925	920	0.038	962	1006
888	867	0.170	862	896	886	0.082	933	960
865	832	0.292	812	840	816	0.219	919	937
816	811	0.043	785	784	757	0.259	863	928
773	746	0.257	727	728	728	0.005	784	887
719	687	0.329	711	628	610	0.216	727	818
603	602	0.009	607	587	579	0.103	607	791
564	561	0.035	580	575	563	0.150	578	770
538	522	0.212	531	521	521	0.000	530	744
503	502	0.003	514	503	503	0.000	514	726
470	470	0.007	499	467	463	0.064	498	703
440	440	0.004	467	442	439	0.033	467	644
425	424	0.014	416	411	410	0.019	416	627
408	406	0.032	403	392	385	0.000	395	607
385	385	0.003	394	385	384	0.141	328	578
369	369	0.000	328	338	337	0.025	313	568
316	315	0.026	313	311	310	0.019	304	531
310	305	0.123	305	287	285	0.046	247	499
282	275	0.178	247	253	252	0.027	227	488
272	269	0.059	228	209	177	1.430	206	467
254	254	0.000	207	140	140	0.004	185	416
126	80	5.221	187	127	127	0.013	177	403
78	76	0.197	176	111	109	0.083	124	393
68	67	0.096	125	92	61	4.507	115	367
63	43	3.940	116	25	24	0.227	99	328
			100					311
								257
								242
								205
								190
								173
								154
								127
								119

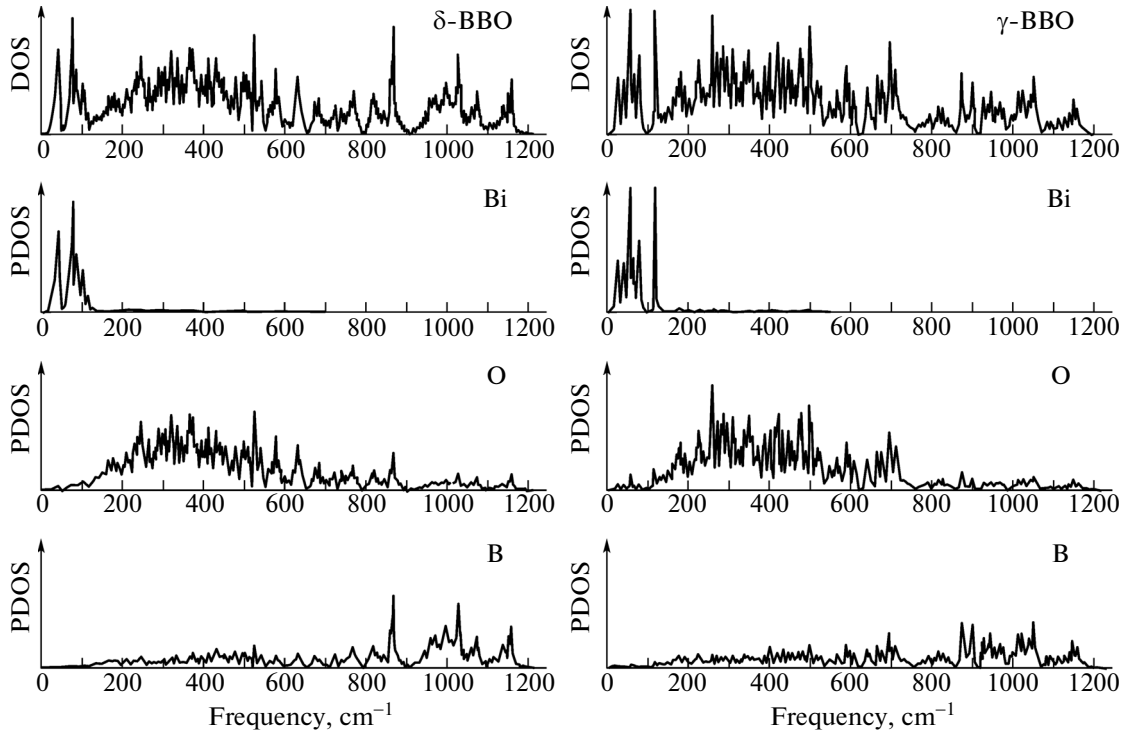

Fig. 1. Densities of phonon states of δ-BBO (at the left) and γ-BBO (at the right): (from top to bottom) the total density of states (DOS) and the partial densities of states (PDOS) of bismuth, oxygen, and boron ions.

$$F_{\text{vibr}}(T) = \int d\omega g(\omega)\left[\frac{\hbar\omega}{2} + k_B T \ln\left(1 - \exp\left(-\frac{\hbar\omega}{k_B T}\right)\right)\right], \quad (5)$$

where E_{static} is the total energy, $E_{\text{vibr}}(T)$ is the vibrational energy consisting of the zero-oscillation energy (first term), and the thermal oscillation energy (second term); and $g(\omega)$ is the density of phonon states.

As is seen from Fig. 1, the densities of phonon states of δ-BBO and γ-BBO demonstrate some differences which are most clearly observed in the partial densities of states. Namely, the partial density of state of bismuth monoclinic phase has a peak near 120 cm^{-1}, while the bismuth vibrations at this frequency are absent in the orthorhombic phase. In high-frequency spectral region, where predominantly boron atoms take part in the vibrations, the differences in the densities of states are insignificant; we can only note that a great number of the vibration frequencies exist in the orthorhombic phase in the range of 800 cm^{-1}–1200 cm^{-1}.

These differences in the densities of phonon states are observed in temperature dependences $F_{\text{vibr}}(T)$ for δ-BBO and γ-BBO shown in Fig. 2. It is seen that the vibrational energy of the γ phase is more favorable than that of the δ phase and has a "stepper" temperature dependence. The inset in Fig. 2 shows the temperature dependence of the difference of the free energies of δ-BBO and γ-BBO; it is seen that the δ-BBO structure is stable below 1100 K, and the γ-BBO structure becomes stable at temperatures higher than 1100 K. The phase transition temperature between the two

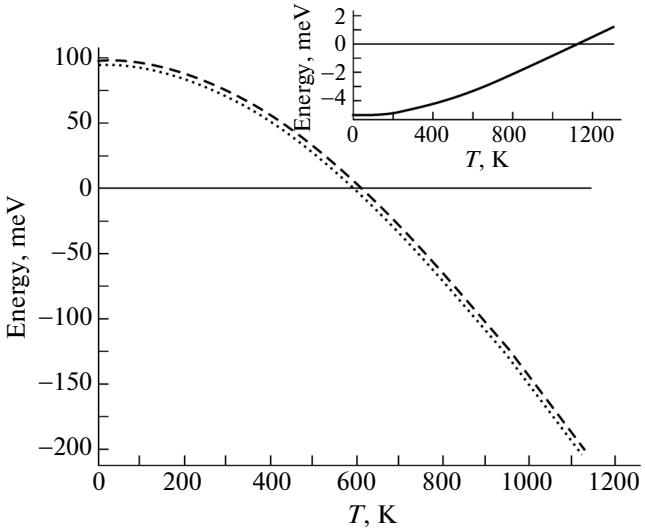

Fig. 2. Temperature dependences of the vibrational energy (Eq. (5)) for δ-BBO (dashed line) and γ-BBO (points). The inset shows the temperature dependence of the difference between the free energies (Eq. (4)) of δ-BBO and γ-BBO.

Table 6. Calculated values of bulk modulus B (GPa), high-frequency permittivity ε_∞^{ii}, and refractive indices n_i for δ-BBO and γ-BBO (the refractive indices obtained in [11, 12] are given in the parentheses)

	γ-BBO	δ-BBO
B, GPa	188.5	201.0
ε_∞^{xx}	3.55	3.55
ε_∞^{yy}	3.47	3.62
ε_∞^{zz}	3.47	3.73
n_x	1.88(2.14)	1.88(2.09)
n_y	1.86(2.06)	1.90(2.11)
n_z	1.86(2.06)	1.93(2.20)

structural modifications calculated in this work agrees well with the experimental value $T = 950$ K [2].

Now, we consider the estimation of the polarization magnitude in δ-BBO. The δ phase of this compound is usually assigned to pyroelectrics, because the phase has no domain structure, and there are no experimental data on the possible polarization switching of the sample when external electric field is applied. As is known, it is impossible to estimate the polarization magnitude of a pyroelectric using the structural data on atomic coordinates in the unit cell, since there is infinite number of variants of choosing the origin of atomic displacements. The estimation can be performed if the structure with the inversion center could

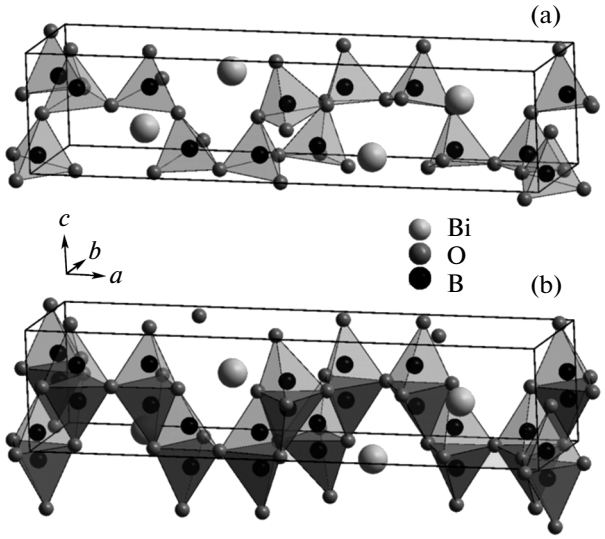

Fig. 3. (a) Structure of δ-BBO with symmetry space group $Pca2_1$ and (b) the structure of the centrosymmetric praphase of δ-BBO with symmetry space group *Pbcm* (in each of tetrahedra, the boron ion occupies its own position with probability of 1/2).

Table 7. Total energies and individual contributions to the energy (eV/at) for δ-BBO and γ-BBO

	δ-BBO	γ-BBO	ΔE
E_{full}	−36.214559	−36.206352	−0.008207
E_{short}	6.818838	6.635765	0.183073
E_{coulomb}	−42.578558	−42.242114	−0.336444
E_{dipole}	−0.305630	−0.429230	0.123600
$E_{\text{quadrupole}}$	−0.149245	−0.170775	0.021530

be obtained using relatively small displacements of the initial structure ions. In δ-BBO, we can displace bismuth and oxygen atoms (Table 1) parallel to crystal axis c, so that they will arranged in plane $z = 0$ (coordinates z of a bismuth ion and each of six oxygen ions will take the value 0). The obtained structure remains polar with the same symmetry space group $Pca2_1$ and also with four molecules in the unit cell. An important specific feature of the structure is the fact that it is possible to finish building of each tetrahedron of the structure to a triangular bipyramid consisting of two tetrahedrons connected by a face perpendicular to axis c of the crystal. The difference between the tetrahedra is that one of them contains a boron ion in its interior, and another does not contain it. Thus, one can be imagined that the basis of this structure is a framework from bipyramids, not tetrahedra, connected to each other by edges or vertices. However, the transfer of each boron ion in the bipyramid from one tetrahedron to another does not change translation and point symmetry of the structure, and only the crystal polarization vector direction is changed to the opposite direction.

It would appear natural to assume that the γ-BBO praphase is a structure, in which boron ion equally probably occupy to positions in the bipyramids (Fig. 3). This structure belongs to nonpolar orthorhombic space group *Pbcm* with four molecules in the unit cell; i.e., the translation symmetry of the crystal is not changed when disordering boron ions over two positions.

The polarization was calculated by formulas

$$P = P_{\text{ion}} + P_{\text{el}}, \tag{6}$$

$$P_{\text{ion}} = \frac{1}{V}\sum_{i=1}^{N} Z_i^{\text{ion}} u_i. \tag{7}$$

Here, N is the number of atoms in the unit cell; V is the unit cell volume; Z_i^{ion} is the nominal charge of the ith ion; u_i is the displacement distance of the ith ion along axis z from the praphase to the polar phase observed experimentally (boron ions were displaced from their mean positions, i.e., from the bipyramid bases); P_{el} is the polarization due to dipole distortions of the electron density of ions. The polarization magnitude was

131 μC/cm^2 with the ionic and electronic contributions 117 μC/cm^2 and 14 μC/cm^2, respectively.

4. CONCLUSIONS

The main results of this study can be summarized as follows.

The total crystal lattice vibration spectrum, the elastic constants, and the high-frequency permittivity of two bismuth triborate modifications δ-BBO and γ-BBO were calculated in terms of the ab initio model of an ionic crystal. The calculated vibration frequencies of the IR- and Raman-active modes in the Brillouin zone center for δ-BBO, and the refractive indices of δ-BBO and γ-BBO agree well with the experimental data.

The calculations showed that the difference between the energies of the γ-BBO and δ-BBO phases at $T = 0$ is 8 meV, and the vibrational contribution to the free energy at all finite temperatures in γ-BBO is energetically more favorable than that in δ-BBO. The calculated temperature of the phase transition from δ-BBO to γ-BBO of 1100 K agrees adequately with the experimental value of 950 K.

We proposed the structure of the nonpolar δ-BBO praphase with disordering of boron ions over two equally probable positions. The polarization of δ-BBO was estimated to be 131 μC/cm^2.

ACKNOWLEDGMENTS

This study was supported by the Council on Grants from the President of the Russian Federation for Support of the "Leading Scientific Schools" (grant no. NSh-924.2014.2).

REFERENCES

1. J. Liebertz, Z. Kristallogr. **158**, 319 (1982).
2. R. H. Cong, J. L. Zhu, Y. X. Wang, T. Yang, F. H. Liao, C. Q. Jin, and J. H. Lin, Cryst. Eng. Commun. **11**, 1971 (2009).
3. R. H. Cong, T. Yang, J. Sun, Y. X. Wang, and J. H. Lin, Inorg. Chem. **52**, 7460 (2013).
4. J. Yang and M. J. Dolg, Phys. Chem. B **110**, 19 254 (2006).
5. Z. S. Lin, Z. Z. Wang, C. T. Chen, and M. H. Lee, J. Appl. Phys. **90**, 5585 (2001).
6. M. Maczka, L. Macalik, and A. J. Majchrowski, Alloys Compd. **575**, 86 (2013).
7. E. G. Maksimov, V. I. Zinenko, and N. G. Zamkova, Phys.—Usp. **47** (11), 1075 (2004).
8. J. S. Knyrim, P. Becker, D. Johrendt, and H. Huppertz, Angew. Chem., Int. Ed. **45**, 8239 (2006).
9. L. Li, G. Li, Y. Wang, F. Liao, and J. Lin, Inorg. Chem. **44**, 8243 (2005).
10. H. T. Stokes and D. M. Hatch, J. Appl. Crystallogr. **38**, 237 (2005).
11. A. V. Cherepakhin, A. I. Zaitsev, A. S. Aleksandrovsky, and A. V. Zamkov, Opt. Mater. **34**, 790 (2012).
12. S. V. Mel'nikova and L. I. Isaenko, Phys. Solid State **54** (10), 1966 (2012).
13. H. Kuzmany, *Solid-State Spectroscopy: An Introduction* (Springer-Verlag, Berlin, 1998).
14. A. A. Maradudin, E. W. Montroll, and G. H. Weiss, *Theory of Lattice Dynamics in the Harmonic Approximation* (Academic, New York, 1963).

Translated by Yu. Ryzhkov